The EMBO Journal Vol.18 No.9 pp.2364–2371, 1999

Tubulin-like protofilaments in Ca^{2+}-induced FtsZ sheets

Jan Löwe[1] and Linda A.Amos

MRC Laboratory of Molecular Biology, Hills Road, Cambridge CB2 2QH, UK

[1]Corresponding author
e-mail: jyl@mrc-lmb.cam.ac.uk

The 40 kDa protein FtsZ is a major septum-forming component of bacterial cell division. Early during cytokinesis at midcell, FtsZ forms a cytokinetic ring that constricts as septation progresses. FtsZ has a high propensity to polymerize *in vitro* into various structures, including sheets and filaments, in a GTP-dependent manner. Together with limited sequence homology, the occurrence of the tubulin signature motif in FtsZ and a similar three-dimensional structure, this leads to the conclusion that FtsZ is the bacterial tubulin homologue. We have polymerized FtsZ1 from *Methanococcus jannaschii* in the presence of millimolar concentrations of Ca^{2+} ions to produce two-dimensional crystals of plane group $P222_1$. Most of the protein precipitates and forms filaments ~23.0 nm in diameter. A three-dimensional reconstruction of tilted micrographs of FtsZ sheets in negative stain between 0 and 60° shows protofilaments of FtsZ running along the sheet axis. Pairs of parallel FtsZ protofilaments associate in an antiparallel fashion to form a two-dimensional sheet. The antiparallel arrangement is believed to generate flat sheets instead of the curved filaments seen in other FtsZ polymers. Together with the subunit spacing along the protofilament axis, a fitting of the FtsZ crystal structure into the reconstruction suggests a protofilamant structure very similar to that of tubulin protofilaments.

Keywords: electron microscopy/FtsZ/*Methanococcus jannaschii*/three-dimensional image reconstruction/two-dimensional crystals

Introduction

Prokaryotic cell division (for recent reviews see Bramhill, 1997; Lutkenhaus and Addinall, 1997; Rothfield and Justice, 1997) has been found to be dependent on a number of genes. Most of the genes have been characterized in the Gram-negative eubacterium *Escherichia coli* and belong to the *fts* family (named after a common phenotype of their mutants characterized by temperature-sensitive filamentous growth; Hirota *et al*., 1968) and include *ftsA*, *ftsI* (PBP3), *ftsL*, *ftsN*, *ftsQ*, *ftsW*, *ftsZ*, *zipA* and others. At present, genomic sequencing of prokaryotes has found that only FtsZ is conserved (Erickson, 1997). Some of the genes essential for cell division in prokaryotes that are enclosed in a cell wall are involved in septal peptidoglycan synthesis and are absent in organisms without a cell wall. FtsZ can be regarded as being ubiquitous in eubacteria and archaea, and has also been found in chloroplasts (Osteryoung and Vierling, 1995) but not in mitochondria. Some archaea contain two different *ftsZ* genes, although nothing is known about their function. Sequence analysis revealed that all such pairs of *ftsZ* genes can be grouped into two different protein families, FtsZ1 and FtsZ2, suggesting two distinct conserved functions (Faguy and Doolittle, 1998).

During cell division, FtsZ assembles into a cytokinetic ring, called the Z-ring (Bi and Lutkenhaus, 1991). The Z-ring is part of the septum that constricts and generates two daughter cells. The precise role of the Z-ring is still enigmatic. Thin sections of the septum show no subassemblies and no microtubule-like polymers. Mutants of FtsZ that form spirals *in vitro* force the septum to be helical *in vivo*, suggesting that FtsZ acts as the structure-forming component of the septum (Addinall and Lutkenhaus, 1996). While the contractile ring of eukaryotic cells consists of actin, FtsZ is probably an ancestral homologue of the eukaryotic tubulins (Erickson, 1995). FtsZ has weak sequence homology to tubulin in the N-terminal two-thirds (de Pereda *et al*., 1996; Nogales *et al*., 1998a), carries the tubulin signature motif GGGTGS/TG, and both proteins are of about the same size of 40–50 kDa. Crystal structures of FtsZ (Lowe and Amos, 1998) and αβ-tubulin in two-dimensional Zn-induced sheets (Nogales *et al*., 1998b) demonstrated that both proteins share the same fold and nucleotide-binding mode. They are more closely related to dinucleotide-binding proteins (Rossmann fold proteins) than to classical GTPases but should be treated as a new family of GTPases (Nogales *et al*., 1998a). More importantly, FtsZ and tubulin appear to share some functional properties. Tubulin forms protofilaments, rings, sheets and microtubules, naturally occurring polymers that provide a track and anchor for many proteins of the cytoskeleton of eukaryotic cells. αβ-tubulin forms a tight dimer and binds two equivalents of GTP, but only β-tubulin is capable of hydrolysing GTP into GDP. αβ-tubulin dimers form so-called protofilaments, i.e. long filaments in which dimers are connected head-to-tail.

The αβ-tubulin crystal structure has been solved using Zn-induced sheets composed of antiparallel protofilaments, and thus provides information about the longitudinal protofilament-forming interaction of tubulin. Tubulin polymerization is GTP dependent, and microtubules show dynamic instability that is regulated by GTP hydrolysis. The nature of FtsZ polymers *in vivo* is unknown; however, *in vitro* experiments demonstrated that FtsZ can be polymerized into protofilaments, sheets and filaments in a GTP-dependent manner (Bramhill and Thompson, 1994; Mukherjee and Lutkenhaus, 1994, 1998; Erickson *et al*., 1996; Yu and Margolin, 1997). Furthermore, FtsZ poly-

merization shows dynamic properties not very different from those of tubulin (Mukherjee and Lutkenhaus, 1998). Many conditions have been reported for polymerization of FtsZ proteins, including the addition of calcium ions, DEAE-dextran and cationic phospholipids, producing a variety of polymeric structures as seen in electron micrographs. An electron microcopic investigation of FtsZ sheets showed that the longitudinal spacing of the FtsZ polymer is very close to the 40 Å spacing found in tubulin protofilaments (Erickson *et al*., 1996).

In this study, we polymerized the hyperthermophilic FtsZ1 protein from the archaeon *Methanococcus jannaschii* to form, for the first time, sheets suitable for three-dimensional image reconstruction. By fitting the crystal structure of FtsZ into a three-dimensional map, we are able to show that FtsZ forms protofilaments identical to the protofilaments consisting of αβ-tubulin.

Results

FtsZ1 from the hyperthermophilic archaeon *M.jannaschii* has been polymerized in the presence of high calcium concentrations in the range of 5–10 mM at room temperature and low pH. Most of the protein forms insoluble aggregates consisting mainly of large filamentous structures that stick to each other. Single 'cable'-like filaments appear to have helical symmetry, as can be seen in electron micrographs of negatively stained specimens (Figure 1G and H). Two helical repeats of 72 and 144 Å are visible in the diffraction image of a straight 'cable'-like filament (Figure 1G and I). After centrifugation of the polymerization products of FtsZ, a small proportion of the protein stays in solution and exclusively forms sheets with an average size of ~0.3×0.8 μm (Figure 1J). When attached to the carbon, sheets tend to fold over, indicating that both sides are identical. Some sheets contain more than one layer. Untilted images in negative stain show cell dimensions of 42.9×139.3 Å and diffract to the second order along *a* and to the eighth order along *b* (Figure 1A–C). The mm symmetry seen in diffraction images of untilted sheets indicates a 2-fold axis along the sheet plane (Figure 1B). After filtering, two symmetrical thick filaments form a unit cell in the *b* direction (Figure 1C). Comparison of phases of symmetry-related reflections indicated the plane group $P222_1$, with the 2-fold screw axis running along *b* (Figure 2A). Quick-frozen FtsZ sheets observed under cryo conditions diffract to slightly higher resolution (Figure 1D–F) but show essentially the same structure as negatively stained images (Figure 1F) with more evidence for connections between filaments.

To obtain three-dimensional information about the structure of polymerized FtsZ, 24 images in the tilt range of 0–60° have been taken in negative stain. Fourier processing (Figure 2B, Table I) yielded a low-resolution map of the filament structure of FtsZ in Ca^{2+}-induced sheets (Figure 3A–C). The structure consists of alternating thick filaments that each contain more than one FtsZ molecule per repeat along the *b* axis. The thick filaments have almost no contact with each other except for regions at the very outer surfaces (top and bottom of Figure 3B). The large gaps between the thick filaments may be exaggerated by the stain since we see more connections in ice-embedded sheets (Figure 1F). The three-dimensional map of FtsZ sheets does not allow an unambiguous placement of individual FtsZ molecules due to the low resolution. One possibility is that FtsZ forms protofilaments in the same way as tubulin.

We constructed a model of a single FtsZ protofilament by superimposing the FtsZ coordinates (Lowe and Amos, 1998) on β-tubulin in the electron crystallographic structure of αβ-tubulin Zn sheets (Nogales *et al*., 1998b). A protofilament was then generated by translating a second FtsZ molecule by 42.9 Å along the protofilament axis (Figure 4). This produces a protofilament where loop T7 in FtsZ comes very close to the nucleotide of the next subunit, as has been observed in tubulin (Nogales *et al*., 1998a,b). Protofilaments constructed in this way have been placed in the three-dimensional map of FtsZ sheets. Two tubulin-like FtsZ protofilaments are needed to fill the density of the thick filaments seen in the reconstructed map (Figure 3A–C). Two FtsZ protofilaments run in parallel to form each thick filament, and two thick filaments, related by 2-fold plane group symmetry, form the unit cell in the *b* direction. The subunit arrangement of paired parallel protofilaments and antiparallel thick filaments results from the plane group symmetry alone. The asymmetric unit contains one molecule of FtsZ. The N-terminal regions of FtsZ monomers point upwards and downwards (Figure 3B and C) and do not fill the density perfectly in this region, indicating that helix H0 might change its position relative to the crystal structure. The C-termini are on the other side of the filaments and form lateral contacts which connect two thick filaments (Figure 3B). There are two types of lateral contacts: very limited contacts connect two thick filaments using the C-terminal residues, and broad contacts form a thick filament from two tubulin-like FtsZ protofilaments. The latter contact is a dimeric contact between two S3 strands of the GTPase domain of FtsZ (Figure 5). This contact is not present in the X-ray crystal structure of FtsZ.

Discussion

We have produced sheets of FtsZ large enough for three-dimensional image reconstruction. The resulting three-dimensional map shows antiparallel thick filaments each with 2-fold rotational symmetry. Two tubulin-like protofilaments of FtsZ constructed from the X-ray crystal structure of FtsZ fit very well into a thick filament. Also taking into account structural analogies that would allow similar contacts in polymers of tubulin and FtsZ proteins, we propose that tubulin and FtsZ use the same mechanism of longitudinal polymerization into protofilaments. Conditions for FtsZ polymerization used in this study deviate greatly from those published for reversible polymerization and depolymerization (Yu and Margolin, 1997; Mukherjee and Lutkenhaus, 1998). The use of a high calcium concentration enabled us to separate other polymers from flat sheets by centrifugation. Calcium signals have been implicated in bacterial cell division, but it remains to be proven that calcium acts directly on FtsZ *in vivo* (Chang *et al*., 1986; Norris, 1989). Most of the protein forms insoluble 'cable'-like structures as seen in the electron microscope (Figure 1G and H). The helical repeats of 72 and 144 Å (Figure 1G and I) are very close to the *b* axis of the FtsZ sheets, suggesting that both structures use a

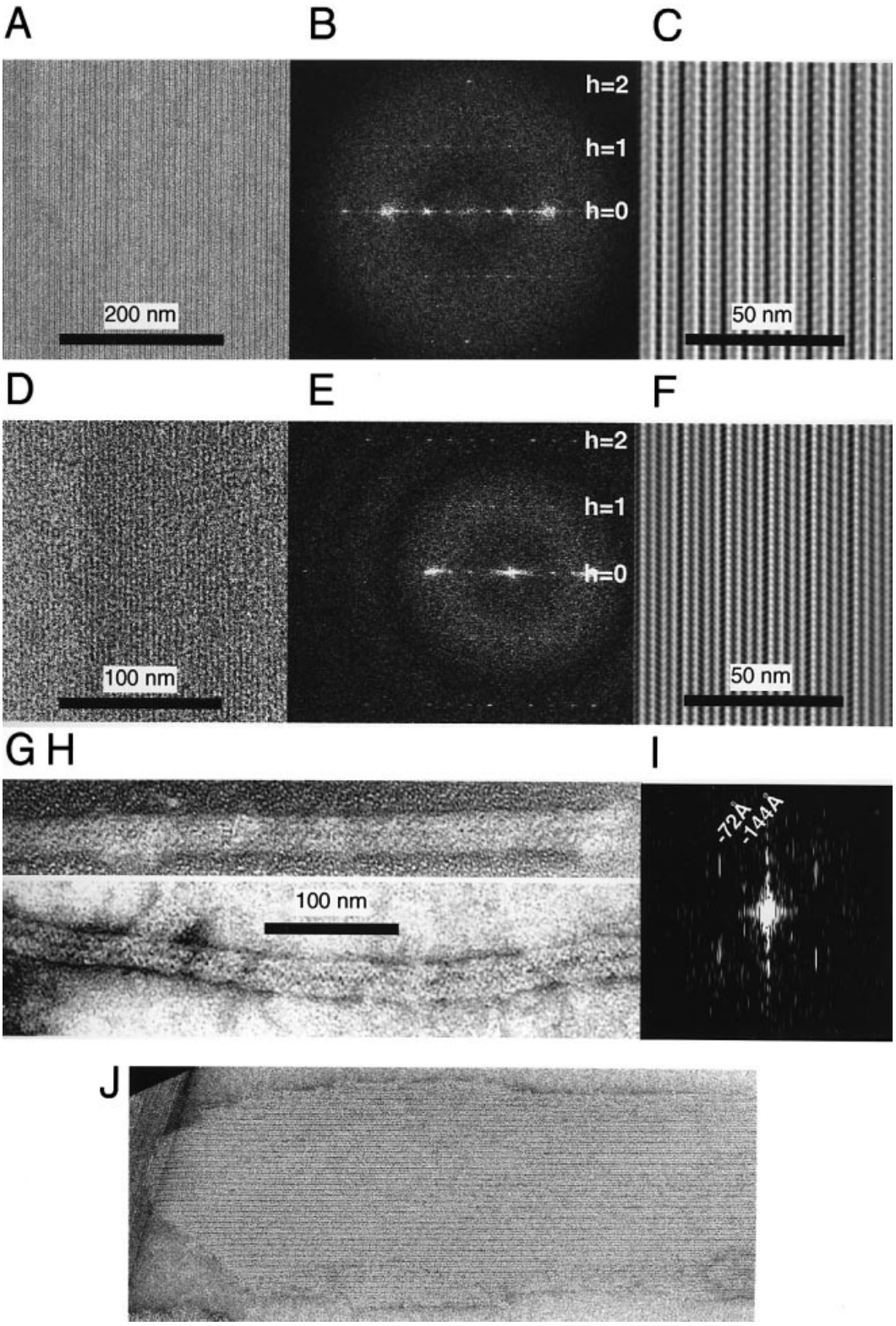

Fig. 1. FtsZ1 from *M.jannaschii* in 20 mM Tris pH 7.5, 1 mM EDTA, 1 mM azide was polymerized for 2–3 h at room temperature by the addition of 8 mM GTP, 8 mM calcium chloride and 8 mM magnesium acetate. After removal of precipitated protein, samples were negatively stained (A–C and J) or quick frozen in liquid ethane (D–F). (**A** and **D**) Untilted images. (**B**) Negatively stained specimens diffract to h = 2 and show mm symmetry when untilted. Cell constants: a = 42.9 Å, b = 139.3 Å. (**C**) A filtered image of the sheet in (A) reveals that the two thick filaments running antiparallel build a unit cell. (**E**) Cryo-preserved sheets diffract to higher resolution, but show the same architecture of twinned filaments in filtered images with four thin filaments in a unit cell. Four thin filaments are in a unit cell (**F**). (**G** and **H**) 'Cable'-like filaments of FtsZ in negative stain. Almost all precipitated protein assembles into these filaments. (**I**) Diffraction image of the filaments shown in (G). Visible repeats of 72 and 144 Å correspond to the *b*-axis of FtsZ sheets. The diffraction pattern indicates helical symmetry for the 'cables'. (**J**) A whole sheet in negative stain.

similar arrangement where two protofilaments dimerize to form a thick filament and where alternating thick filaments are oriented differently. Sheets had to be selected by eye in the electron microscope to obtain enough images because most sheets formed twisted ribbons with both sides attached to the carbon; both sides of the sheets are chemically identical due to plane group symmetry.

Because of the low yield of suitable sheets, this study was limited to negative stain, but a projection image of an FtsZ sheet under cryo conditions shows essentially the same features as the negatively stained specimens. The three-dimensional reconstruction shows thick, dimeric filaments running antiparallel. Even if there was a bending force built into individual protofilaments (as has been seen by others), then this arrangement could produce flat sheets by balancing two opposite bending forces. A similar arrangement has been seen in αβ-tubulin Zn sheets where individual protofilaments run antiparallel (Baker and Amos, 1978; Nogales *et al*., 1998b). The three-dimensional reconstruction has a nominal resolution of a ~15 Å in plane and ~30 Å perpendicular to the plane of the sheet. At that resolution, it is not possible to fit individual FtsZ subunits into the density. However, there is compelling evidence that FtsZ forms longitudinal contacts very similar to those of tubulin. First, sheets of FtsZ described here and elsewhere (Erickson *et al*., 1996) show the characteristic ~40 Å longitudinal repeat of tubulin protofilaments, although the spacing is slightly greater (42.9 Å versus 40.0 Å for tubulin Zn sheets). Furthermore, tubulin uses loop T7 to make a very important longitudinal contact into the active site of a downstream subunit in the protofilament. Loop T7 comes very close to the nucleotide of the next subunit and has been implicated in polymerization-dependent GTPase activation. A possible mechanism involves the strictly conserved residue Glu254 in loop T7 of α-tubulin and the corresponding, strictly conserved residue Lys254 in β-tubulin. Glu254 reaches into the active site of β-tubulin in a protofilament and activates the GTPase acitivity of β-tubulin (Nogales *et al*., 1998a). The same loop in β-tubulin with Lys254 is incapable of GTPase activation and renders α-tubulin inactive. Loop T7 in FtsZ is the only region not directly involved in nucleotide binding that has sequence homology to tubulin and would reach the nucleotide of a downstream subunit in a tubulin-like protofilament of FtsZ (Figure 4A–C). Importantly, an Asp212Ala mutation in *E.coli* FtsZ (Asp238 in *M.jannaschii* FtsZ1), which is in loop T7, abolishes GTP hydrolysis but not GTP binding (Dai *et al*., 1994). Loop T7 is not in the active site of the monomer but on the opposite surface of the molecule, suggesting that T7 facilitates polymerization-dependent GTPase activation in FtsZ as well. Finally, the two surfaces assumed to form the longitudinal contacts in the FtsZ protofilament are complementary to each other, with only minor side chain clashes. Residues in the loop between H6 and H7 collide with residues in H10; loop S3/H3 is too close to the end of H0. A minor collision involves loop S3/H3 and loop T7.

In the three-dimensional reconstruction of FtsZ sheets, two FtsZ protofilaments model nicely a thick filament in one orientation only. A large gap between thick filaments

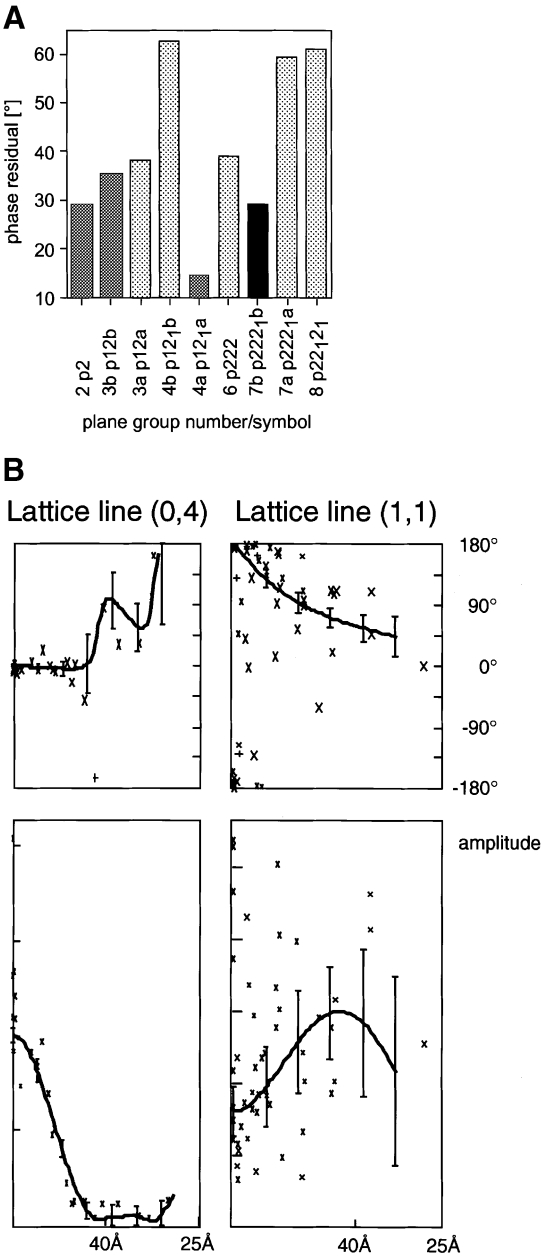

Fig. 2. (**A**) A graphic representation of plane group determination results. Phase residuals as produced by the program ALLSPACE for all plane groups compatible with cell constants and cell angles. a and b give the direction of the second symmetry operator in plane group names. P222$_1$b and the sub-groups P2, P12b and P12$_1$a produce low residuals. (**B**) Lattice line fitting for the two structure factors *F*(0,4) and *F*(1,1). Twenty four images in the tilt range 0–60° were used. Top, lattice line fitting for the continuous phase; bottom, lattice line fitting for the continuous amplitude.

Table I. Electron microscopy data

Plane group	P222$_1$ (7)
Unit cell dimensions	42.9 ×139.3 Å thickness: ~100 Å
No. of images	24
Tilt range	0–60°
Underfocus	500–800 nm
Merged *I*/α	626
Unique *F*s	80
IQ cut-off	6
Resolution in plane	~15 Å (nominal)
Phase residual	30.2°
R-factor	0.38

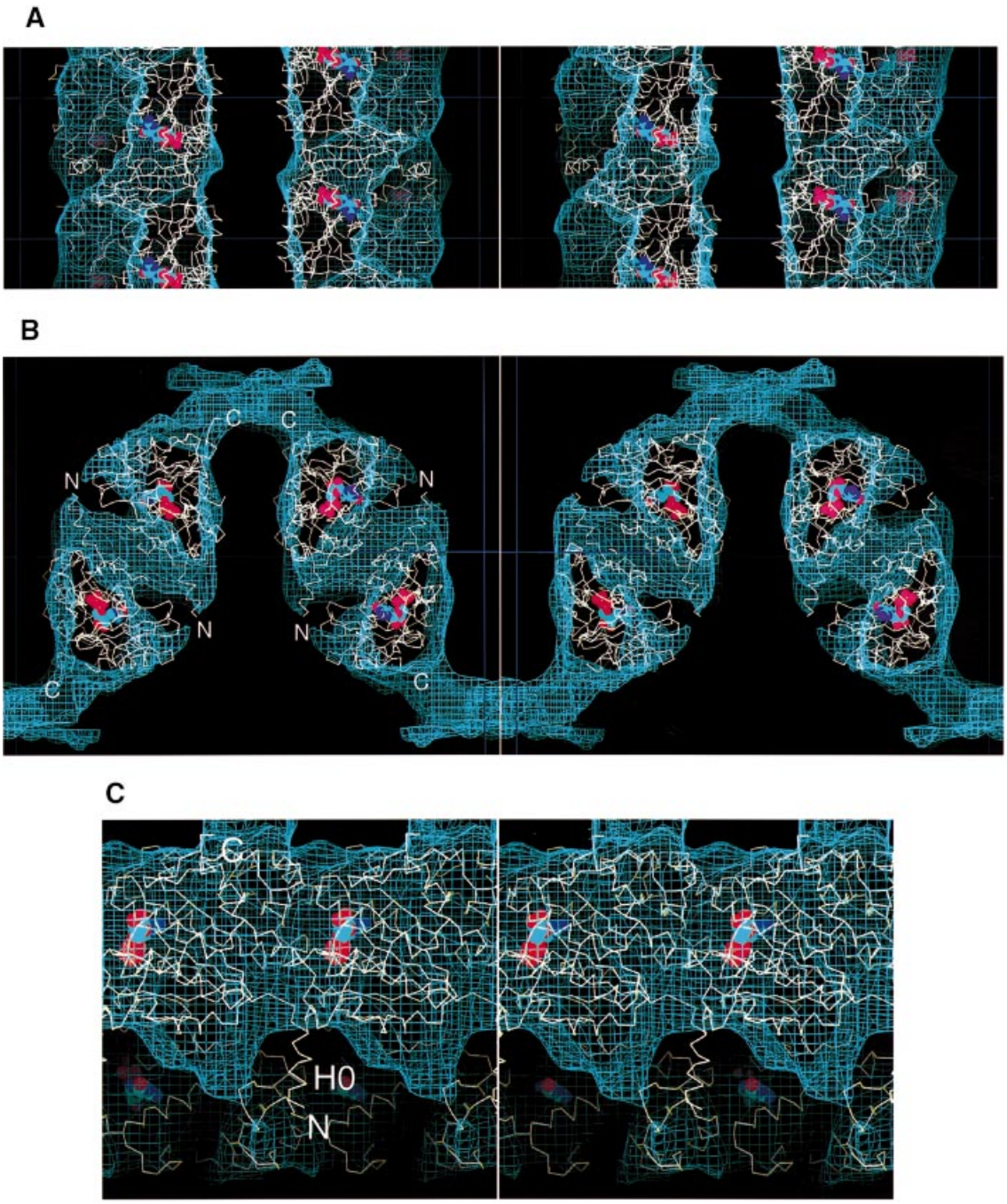

Fig. 3. Stereo plots of the three-dimensional map of Ca^{2+}-induced FtsZ sheets with manually fitted FtsZ protofilaments. Atomic coordinates are represented by C_α positions only, and GDP is drawn as spheres. (**A**) Two antiparallel thick filaments form the unit cell. Large, stain-filled gaps separate thick filaments. (**B**) Thick filaments consist of two FtsZ protofilaments running parallel. The gaps between thick filaments can be bridged by C-terminal residues of FtsZ that are disordered in the X-ray crystal structure. (**C**) Side view of a single FtsZ protofilament fitted into the three-dimensional reconstruction of FtsZ sheets. Helix H0 sticks out of the density but extra density suggests that it may fold onto the surface of the same or next monomer. The position of helix H0 in the X-ray crystal structure used for generating the protofilament model of FtsZ is determined by crystal contacts that are not present in the sheets (Lowe and Amos, 1998). Prepared with MAIN (Turk, 1992).

could be bridged by C-terminal residues (357–372; Figure 3B) that are partly disordered in the X-ray crystal structure but form a dimeric contact there too (not shown). The N-terminal helix H0 does not fit into the density but could be moved to fill the only empty part of the density which lies nearby (Figure 3C). Helix H0 is not part of the otherwise compact structure in the three-dimensional crystal, and its position is determined by crystal contacts only (Lowe and Amos, 1998). Residues 1–22, partly disordered in the crystal structure, could also fit into the empty density of the electron microscopy map (Figure 3C). The tubulin protofilament structure gives no indication of helix H0's position because tubulin starts with strand S1 and has no helix H0. In the sheets, two GTPase domains of FtsZ bind to each other mainly via a dimer contact between S3 strands to form thick filaments from protofilaments (Figure 5). This interaction may be calcium dependent as it has not been seen before. Comparison

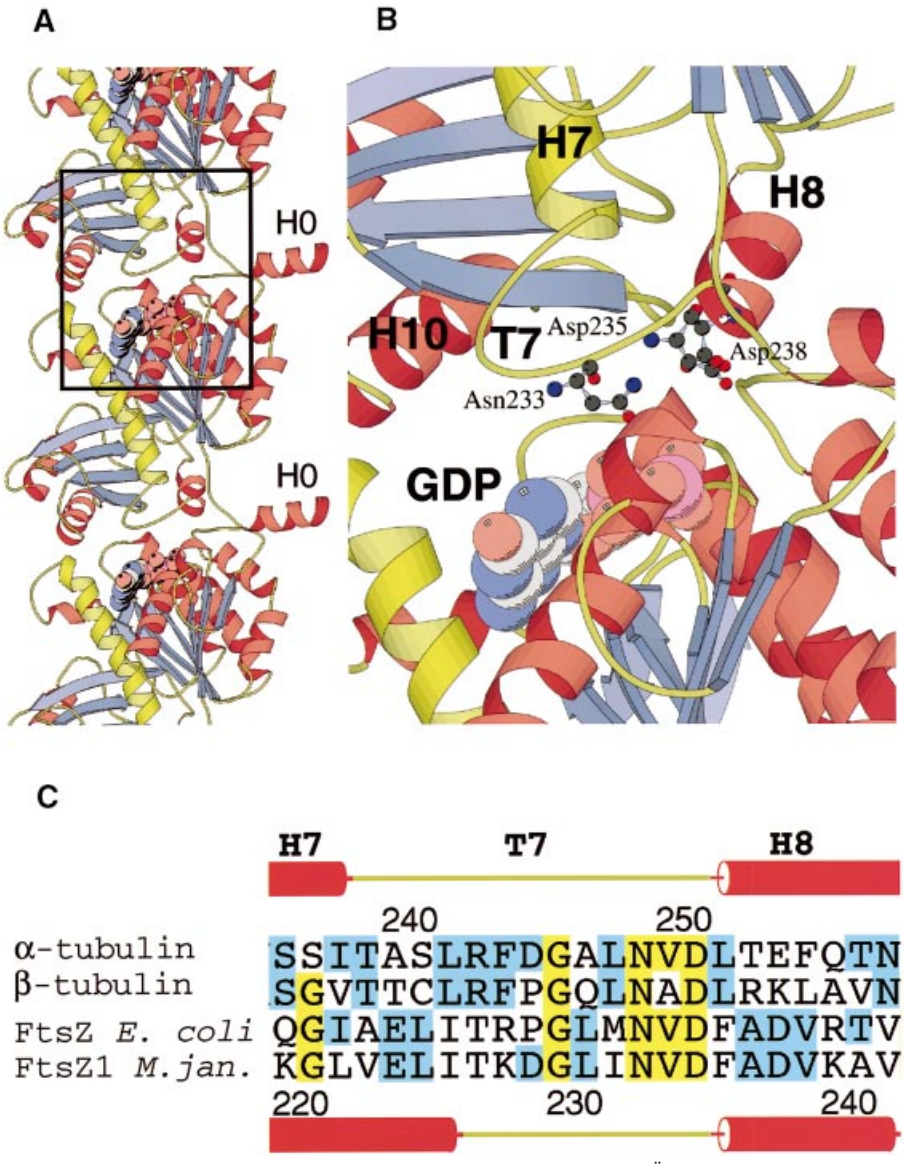

Fig. 4. Model of the FtsZ protofilament used in Figure 3. (**A**) FtsZ (PDB accession code 1FSZ, Lowe and Amos, 1998) was oriented according to β-tubulin in the three-dimensional reconstruction of αβ-tubulin Zn sheets (PDB accession code 1TUB; Nogales *et al*., 1998b). A protofilament was constructed by adding FtsZ molecules displaced by the repeat in FtsZ sheets (42.9 Å). (**B**) Detailed view of the region around loop T7, rotated by 20° around the *y*-axis for clarity. Loop T7 reaches into the active site of a downstream subunit. Loop T7 in tubulin has been implicated in polymerization-dependent activation of GTPase activity (Erickson, 1998; Nogales *et al*., 1998a). Prepared with MOLSCRIPT (Kraulis, 1991). (**C**) Multiple sequence alignment of pig α- and β-tubulin (SWISS_PROT:TBA_PIG, TBB_PIG), *E.coli* FtsZ (SWISSPROT: FTSZ_ECOLI) and FtsZ1 from *M.jannaschii* (SWISSPROT:FTS1_METJA). Residues conserved in three or all sequences are shown in yellow; residues conserved in two sequences are shown in light blue. Loop T7 contains many conserved residues including the potentially GTPase-activating acidic residue Asp238 (Asp212 in *E.coli*) (Nogales *et al*., 1998a). Lys254 in β-tubulin would render α-tubulin inactive when α- and β-tubulin form a protofilament. Prepared with ALSCRIPT (Barton, 1993).

with the lateral interactions between tubulin protofilaments both in Zn-induced sheets and in microtubules (Nogales *et al*., 1999) reveals no similarities. FtsZ shows the same behaviour as tubulin in forming very tight longitudinal contacts to give protofilaments. Protofilaments associate through much weaker lateral contacts. It seems that FtsZ can assemble into a multitude of different polymers using different lateral contacts.

In conclusion, it has been shown that the protofilaments formed by FtsZ are completely homologous to tubulin protofilaments in their longitudinal contacts, extending the homology between tubulin and FtsZ to the polymerization-dependent GTPase activation mechanism. We believe that the conserved longitudinal contacts are part of the *in vivo* FtsZ polymer, but it remains to be seen what lateral contacts FtsZ uses to form the Z-ring.

Materials and methods

FtsZ1 from *M.jannaschii* (SWISSPROT:FTZ1_METJA) has been expressed in *E.coli* and purified as published (Lowe and Amos, 1998). The expressed protein contains all 364 residues of the native full-length proteins plus eight residues at the C-terminus (GSHHHHHH).

For polymerization, 8 mM magnesium acetate, 8 mM calcium chloride and 8 mM (neutralized) GTP were added to FtsZ1 in 20 mM Tris pH 7.5, 1 mM EDTA, 1 mM azide to give a final protein concentration of 2 mg/ml. Most protein precipitates immediately. The pH drops to

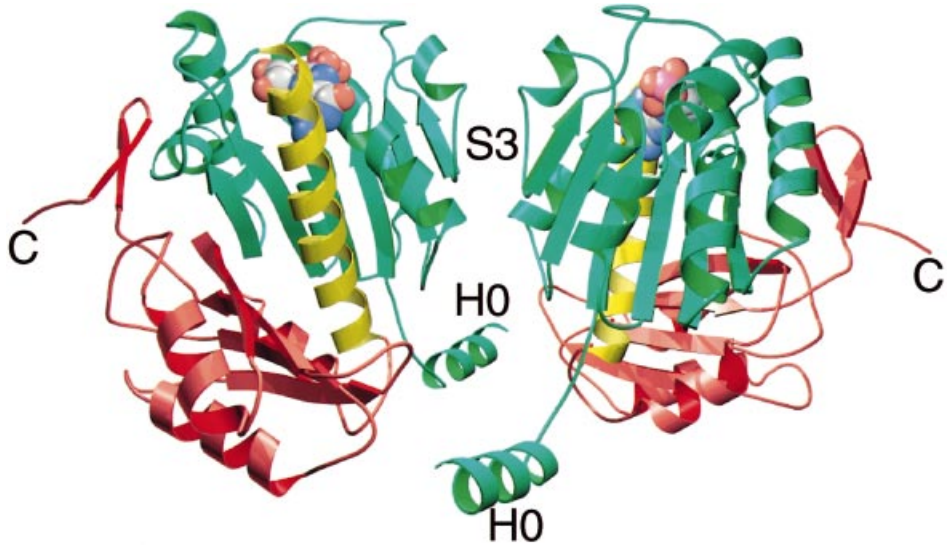

Fig. 5. Dimer contact of two FtsZ molecules forming a thick filament. The outermost region of the strand of the GTPase domain (S3) forms the contact. Prepared with MOLSCRIPT (Kraulis, 1991).

6.0–6.1. After 2–3 h at room temperature without shaking or stirring, precipitated protein was removed by centrifugation and the supernatant was applied to carbon-coated copper grids for electron microscopy. Grids were blotted, stained with 1% uranyl acetate, blotted again and dried for 60 min. Grids were observed at room temperature in a Philips CM12 electron microscope operated at 120 kV. Flat sheets (~0.1%) were selected by eye, and images of 1–2 s were taken at a nominal magnification of 60 000× on Kodak SO-163 film and developed for 10 min in full-strength Kodak D19.

Twenty four micrographs out of 200 in the tilt range of 0–60° were selected and scanned on a Zeiss SCAI scanner with a 28 μm step size. Images were processed with the MRC image-processing programs (Crowther *et al*., 1996). Phase comparison of symmetry-related reflections indicated $P222_1$ symmetry, with the screw axis running across the visible filament axis (crystallographic axis *b*; Figure 2A) The correct choice of symmetry was confirmed later by calculating density functions with subsets of $P222_1$b symmetry: P2, P12b, $P12_1$a. All four calculations produced the same filament arrangement. After two cycles of unbending and correction for the contrast transfer function, amplitudes and phases from 24 images were merged. No refinement of the tilt axes or tilt angles was performed. Merging and refinement details are summarized in Table I. The handedness was determined using the procedure described in Amos *et al.* (1982). A three-dimensional density map was calculated with the CCP4 program suite (Collaborative Computational Project, 1994) with no temperature factor correction.

For the placement of the FtsZ filament in the map, coordinates from FtsZ1 from *M.jannaschii* (PDB: 1FSZ; Lowe and Amos, 1998) were superimposed on the β-tubulin coordinates as determined by electron crystallography (PDB: 1TUB; Nogales *et al*., 1998b). Identically oriented FtsZ1 molecules were added along the filament axis using the 42.9 Å repeat of the FtsZ sheets. One FtsZ protofilament model generated in this way was fitted manually into the three-dimensional map of the FtsZ sheets using MAIN (Turk, 1992), generating all four protofilaments per unit cell by plane group symmetry.

For cryo-electron microscopy, grids were blotted for 5 s and then quick frozen in liquid ethane and transferred at liquid nitrogen temperature into a Gatan cryotransfer specimen holder. Low dose images were taken at zero tilt angle and scanned and processed as described above, using a 7 μm stepsize. Microtubules and αβ-tubulin Zn sheets were used as magnification standards.

Acknowledgements

We would like to thank Keiko Hirose (National Institute for Advanced Interdisciplinary Research, Japan) for help with cryo-electron microscopy, and Juan Fan for providing tubulin Zn sheets. Many thanks to Richard Henderson (MRC-LMB) and Nikolaus Grigorieff for help with image processing. J.L. was supported by an EMBO long-term fellowship.

References

Addinall,S.G. and Lutkenhaus,J. (1996) FtsZ-spirals and -arcs determine the shape of the invaginating septa in some mutants of *Escherichia coli*. *Mol. Microbiol*., **22**, 231–237.

Amos,L.A., Henderson,R. and Unwin,P.N.T. (1982) Three-dimensional structure determination by electron microscopy of two-dimensional crystals. *Prog. Biophys. Mol. Biol*., **39**, 183–231.

Baker,T.S. and Amos,L.A. (1978) The two-dimensional structure of the tubulin dimer in zinc-induced sheets. *J. Mol. Biol*., **123**, 86–106.

Barton,G.J. (1993) ALSCRIPT: a tool to format multiple sequence alignments. *Protein Eng.*, **6**, 37–40.

Bi,E.F. and Lutkenhaus,J. (1991) FtsZ ring structure associated with division in *Escherichia coli*. *Nature*, **354**, 161–164.

Bramhill,D. (1997) Bacterial cell division. *Annu. Rev. Cell Dev. Biol.*, **13**, 395–424.

Bramhill,D. and Thompson,C.M. (1994) GTP-dependent polymerization of *Escherichia coli* FtsZ protein to form tubules. *Proc. Natl Acad. Sci. USA*, **91**, 5813–5817.

Chang,C.F., Shuman,H. and Somlyo,A.P. (1986) Electron probe analysis, X-ray mapping and electron energy-loss spectroscopy of calcium, magnesium and monovalent cations in log-phase and in dividing *Escherichia coli* cells. *J. Bacteriol.*, **167**, 935–939.

Collaborative Computational Project, No. 4 (1994) The CCP4 suite: programs for protein crystallography. *Acta Crystallogr.*, **D50**, 760–763.

Crowther,R.A., Henderson,R. and Smith,J.M. (1996) MRC image processing programs. *J. Struct. Biol*., **116**, 9–16.

Dai,K., Mukherjee,A., Xu,Y. and Lutkenhaus,J. (1994) Mutations in FtsZ that confer resistance to SulA affect the interaction of FtsZ with GTP. *J. Bacteriol.*, **176**, 130–136.

de Pereda,J.M., Leynadier,D., Evangelio,J.A., Chacon,P. and Andreu,J.M. (1996) Tubulin secondary structure analysis, limited proteolysis sites and homology to FtsZ. *Biochemistry*, **35**, 14203–14215.

Erickson,H.P. (1995) FtsZ, a prokaryotic homolog of tubulin? *Cell*, **80**, 367–370.

Erickson,H.P. (1997) FtsZ, a tubulin homologue in prokaryote cell division. *Trends Cell Biol.*, **7**, 362–367.

Erickson,H.P. (1998) Atomic structures of tubulin and FtsZ. *Trends Cell Biol.*, **8**, 133–137.

Erickson,H.P., Taylor,D.W., Taylor,K.A. and Bramhill,D. (1996) Bacterial cell division protein FtsZ assembles into protofilament sheets and minirings, structural homologs of tubulin polymers. *Proc. Natl Acad. Sci. USA*, **93**, 519–523.

Faguy,D.M. and Doolittle,W.F. (1998) Cytoskeletal proteins: the evolution of cell division. *Curr. Biol.*, **8**, R338–R341.

Hirota,Y., Ryter,A. and Jacob,F. (1968) Thermosensitive mutants of *E.coli* affected in the process of DNA synthesis and cell division. *Cold Spring Harbor Symp. Quant. Biol*., **33**, 677–694.

Kraulis,P.J. (1991) MOLSCRIPT: a program to produce both detailed

and schematic plots of protein structures. *J. Appl. Crystallogr.*, **24**, 946–950.
Lowe,J. and Amos,L.A. (1998) Crystal structure of the bacterial cell-division protein FtsZ. *Nature*, **391**, 203–206.
Lutkenhaus,J. and Addinall,S.G. (1997) Bacterial cell division and the Z-ring. *Annu. Rev. Biochem.*, **66**, 93–116.
Mukherjee,A. and Lutkenhaus,J. (1994) Guanine nucleotide-dependent assembly of FtsZ into filaments. *J. Bacteriol.*, **176**, 2754–2758.
Mukherjee,A. and Lutkenhaus,J. (1998) Dynamic assembly of FtsZ regulated by GTP hydrolysis. *EMBO J.*, **17**, 462–469.
Nogales,E., Downing,K.H., Amos,L.A. and Lowe,J. (1998a) Tubulin and FtsZ form a distinct family of GTPases. *Nature Struct. Biol.*, **5**, 451–458.
Nogales,E., Wolf,S.G. and Downing,K.H. (1998b) Structure of the αβ-tubulin dimer by electron crystallography. *Nature*, **391**, 199–203.
Nogales,E., Whittaker,M., Milligan,R.A. and Downing,K.H. (1999) High-resolution model of the microtubule. *Cell*, **96**, 79–88.
Norris,V. (1989) A calcium flux at the termination of replication triggers cell division in *Escherichia coli*. *Cell Calcium*, **10**, 511–517.
Osteryoung,K.W. and Vierling,E. (1995) Conserved cell and organelle division. *Nature*, **376**, 473–474.
Rothfield,L.I. and Justice,S.S. (1997) Bacterial cell division: the cycle of the ring. *Cell*, **88**, 581–584.
Turk,D. (1992) Weiterentwicklung eines Programms fur Molekulgrafik und Elektrondichte-Manipulation und seine Anwendung auf verschiedene Protein-Strukturaufklarungen. PhD thesis, Technische Universitat Munchen, Germany.
Yu,X.C. and Margolin,W. (1997) Ca^{2+}-mediated GTP-dependent dynamic assembly of bacterial cell division protein FtsZ into asters and polymer networks *in vitro*. *EMBO J.*, **16**, 5455–5463.

Received December 23, 1998; revised and accepted March 8, 1999